BIOCHEMISTRY

 Volume 46, Number 20 May 22, 2007

Articles

Binding of a Second Magnesium Is Required for ATPase Activity of RadA from *Methanococcus voltae*†

Xinguo Qian, Yujiong He, and Yu Luo*

Department of Biochemistry, University of Saskatchewan, A3 Health Sciences Building, 107 Wiggins Road, Saskatoon, Saskatchewan, Canada S7N 5E5

Received November 21, 2006; Revised Manuscript Received February 2, 2007

ABSTRACT: RecA-like strand exchange proteins, which include closely related archaeal Rad51/RadA and eukaryal Rad51 and DMC1, play a key role in DNA repair by forming helical nucleoprotein filaments which promote a hallmark strand exchange reaction between homologous DNA substrates. Our recent crystallographic studies on a RadA recombinase from *Methanococcus voltae* (MvRadA) have unexpectedly revealed a secondary magnesium at the subunit interface ~11 Å from the primary one coordinated by ATP and the canonical P-loop. The DNA-dependent ATPase activity of MvRadA appears to be dependent on the concentration of free Mg^{2+}, while the strand exchange activity does not. We also made site-directed mutagenesis at the Mg^{2+}-liganding residue Asp-246. The mutant proteins exhibited ~20-fold reduced ATPase activity but normal strand exchange activity. Structurally, the main chain carbonyl of the conserved catalytic residue Glu-151 is hydrogen bonded with one of the magnesium-liganding water molecules. Changes in the secondary magnesium site may therefore induce conformational changes around this catalytic glutamate and affect the ATPase activity without significantly altering the stability of the extended recombinase filament. Asp-246 is somewhat conserved among archaeal and eukaryal homologues, implying some homologues may share this allosteric site for ATPase function.

RecA-like recombinases facilitate a central DNA strand exchange between a single-stranded DNA (ssDNA)[1] and a homologous double-stranded DNA (dsDNA) in homologous recombination. These recombinases appear to be essential by playing pivotal roles in repair of double-stranded DNA breaks and restart of stalled replication forks (*1*−*5*). This recombinase superfamily (*6*) is composed of bacterial RecA (*7*), archaeal RadA or Rad51 (*8*), and eukaryal Rad51 (*9*) and meiosis-specific DMC1 (*10*). Despite large differences in their primary structures, recent electron microscopic and crystallographic results have revealed strikingly similar "active" recombinase assemblies (*11*−*13*). Such filamentous assemblies are classic allosteric systems equipped with at least two functional sites, one located at subunit interface for binding and hydrolyzing ATP and the other located near the filament axis for binding DNA and promoting strand exchange. In addition to the primary magnesium site which

† This work is supported by SHRF Establishment Grant 1425, NSERC Discovery Grant 161981-03, and CIHR and SHRF Operating Grant 63860. Y.L. is a recipient of CIHR New Investigator Salary Award.

* Corresponding author. Telephone: 1-306-966-4379. Fax: 1-306-966-4390. E-mail: yu.luo@usask.ca.

[1] Abbreviations: MvRadA, RadA recombinase from *Methanococcus voltae*; EcRecA, RecA recombinase from *Escherichia coli*; ssDNA, single-stranded DNA; dsDNA, double-stranded DNA; hdDNA, heteroduplex DNA; ATP, adenosine 5′-triphosphate; ADP, adenosine 5′-diphosphate; AMP-PNP, 5′-adenylyl imidodiphosphate, a nonhydrolyzable analogue of ATP; ATP-γ-S, adenosine 5′-*O*-(3-thiotriphosphate), a slowly hydrolyzable analogue of ATP.

10.1021/bi6024098 CCC: $37.00
Published on Web 04/25/2007

bridges ATP and the canonical P-loop, our recent crystal structures of MvRadA have revealed a secondary magnesium site at the subunit interface. It is worth noting that optimal strand exchange activity of RecA from *Escherichia coli* (EcRecA) has a marked dependence on free Mg^{2+} concentration (*14*). On the other hand, excessive concentration of Mg^{2+} over ATP appears to downregulate strand exchange activity of human Rad51 (*15*). A recent study on human Rad51 has further demonstrated that the recombinase favors binding ATP over ADP at lower Mg^{2+} concentration (*16*). Interestingly, the magnesium-liganding Asp-246 of MvRadA is conserved in human and yeast Rad51 proteins while substituted for a Glu in human and yeast DMC1 proteins. A similar secondary divalent cation-binding site may also exist in some of these eukaryal homologues, which would make MvRadA a prototype for studying the allosteric effects exhibited by its close eukaryal homologues. We set out to study its biochemical implication by studying ATPase and DNA strand exchange activities of wild-type MvRadA and mutant proteins with substitution at Asp-246. Our data suggest that the secondary Mg^{2+} site is important for modulating the ATPase activity of MvRadA.

EXPERIMENTAL PROCEDURES

Cloning, Protein Preparation, and Crystallization. RadA from *Methanococcus voltae* was subcloned into pET28a (Novagen). All site-directed mutations have been introduced by mutagenic primers used in the PCR steps using the overlap extension protocol (*17*, *18*). All resulting plasmids were verified by DNA sequencing using T7 promoter and terminator primers. The recombinant proteins were overexpressed in BL21(DE3)-Codon+RIL cells (Stratagene) and purified as reported (*13*, *19*). In brief, the purification procedure involved steps of polymin P (Sigma) precipitation, high salt extraction, and three chromatography steps using heparin (Amersham Biosciences), hydroxyapatite (Bio-Rad), and DE52 anion-exchange (Whatman) columns. The RadA proteins were concentrated to ~30 mg/mL by ultrafiltration. The crystallization condition for the D246A protein was similar to that of the wild-type MvRadA (Supporting Information).

Single-Stranded DNA-Dependent ATPase Assay. A solution containing 0.033% w/v Malachite Green, 1.3% (w/v) ammonium molybdate, and 1.0 M HCl was used to monitor the release of inorganic phosphate (*20*) from ATP hydrolysis. Absorbance at 620 nm was recorded for quantification. The reaction solutions for the DNA-dependent ATPase assay contained 3 μM RadA, 18 μM ssDNA (in nucleotides), 5 mM ATP, 0.05 M Tris−Hepes buffer at pH 7.4, 100 mM KCl, varied amounts of $MgCl_2$, and 0.1% (v/v) 2-mercaptoethanol. A 36-nt oligonucleotide poly$(dT)_{36}$ (Integrated DNA Technologies) was used as the ssDNA substrate in this assay.

Strand Exchange Assay Using Synthetic Oligonucleotides. The DNA substrates were derived from a published study (*21*). Three oligonucleotides (2, 63 nt, TCCTT TTGAT AAGAG GTCAT TTTTG CGGAT GGCTT AGAGC TTAAT TGCTG AATCT GGTGC TGT, 45A, 36 nt, ACAGC ACCAG ATTCA GCAAT TAAGC TCTAA GCCATG, and 55A, 36 nt, GATGG CTTAG AGCTT AATTG CTGAA TCTGG TGCTGT) were obtained from Integrated DNA Technologies. Equal molarities of complementary oligonucleotides 45A and 55A were heated at 95 °C for 5 min and then slowly cooled to 21 °C to generate the 36-bp dsDNA substrate. The strand exchange solution was composed of 5 mM ATP or an analogous nucleotide, varied amounts of $MgCl_2$, 100 mM KCl, 50 mM Hepes−Tris buffer at pH 7.4, 21 μM MvRadA, 0.1% (v/v) 2-mercaptoethanol, and 1 μM oligonucleotides. The 63-nt ssDNA substrate (oligonucleotide 2) was preincubated at 37 °C with MvRadA for 1 min before the 36-bp dsDNA substrate was added. The reaction was stopped at 30 min by adding EDTA to a concentration of 20 mM and trypsin to a concentration of 1 μg/μL. After 10 min of trypsin digestion, a 10 μL sample was mixed with 5 μL of a loading buffer composed of 30% glycerol and 0.1% bromophenol blue and then loaded onto a 17% acrylamide vertical gel. The SDS−PAGE was developed for 1 h at 100 V and then stained with ethidium bromide. The fluorescent emission by DNA-absorbed ethidium bromide was recorded with a Kodak GelLogic 200 system. Strand exchange yields were quantified using the Kodak MI software, and a reference lane was loaded with a thermally annealed 63-nt/36-nt heteroduplex DNA, a species identical to the strand exchange product.

Strand Exchange Assay Using Virion DNAs. Circular single-stranded ϕX174 virion DNA (5386 nucleotides) and its homologous double-stranded ϕX174 replication form I DNA (5386 base pairs) were purchased from New England Biolabs. The double-stranded replication form I DNA was linearized by *Pst*I (VWR) digestion and purified using a Qiaquick kit (Qiagen) before being used as the dsDNA substrate. The reaction solutions had the same chemical composition as those used in strand exchange between synthetic oligonucleotides. Only ATP was used in this assay. The reaction solution was also supplemented with an ATP-regenerating system composed of 4 mM creatine phosphate and 0.01 unit/μL creatine kinase (VWR). The circular single-stranded ϕX174 virion DNA (5 ng/μL or 15 μM in nucleotides) and MvRadA (5 μM) were first incubated in the reaction buffer at 37 °C for 3 min. Then single-stranded DNA-binding protein (SSB) from *E. coli* (VWR) was added to a concentration of 1 μM. After a second incubation at 37 °C for 3 min, the *Pst*I-linearized dsDNA was added to a concentration of 10 ng/μL (15 μM in base pairs). After a third incubation at 37 °C for 90 min, SDS (a final concentration of 1%) and proteinase K (a final concentration of 1 μg/μL) were added to the reaction solution. A further incubation for 10 min was required to fully degrade MvRadA. A 10 μL sample was mixed with 5 μL of loading buffer composed of 30% glycerol and 0.1% bromophenol blue and loaded onto a 0.6% agarose horizontal gel. The DNA gel electrophoresis was developed for 4 h at a constant electric field of 4 V/cm. The ethidium bromide-stained gel was recorded with the Kodak GelLogic 200 system.

RESULTS

Mg^{2+} Sites in Crystallized MvRadA Filaments. Our recent crystallographic study (*13*) on MvRadA has unexpectedly revealed a secondary Mg^{2+} site as well as a canonical P-loop and nucleotide-lined primary Mg^{2+} site (Figure 1). Besides, a promiscuous pocket for binding either two K^+ (*22*) or one Ca^{2+} (*23*) has been found as a plausible structural basis of cationic stimulation on Rad51 orthologues (Figure 1). Both

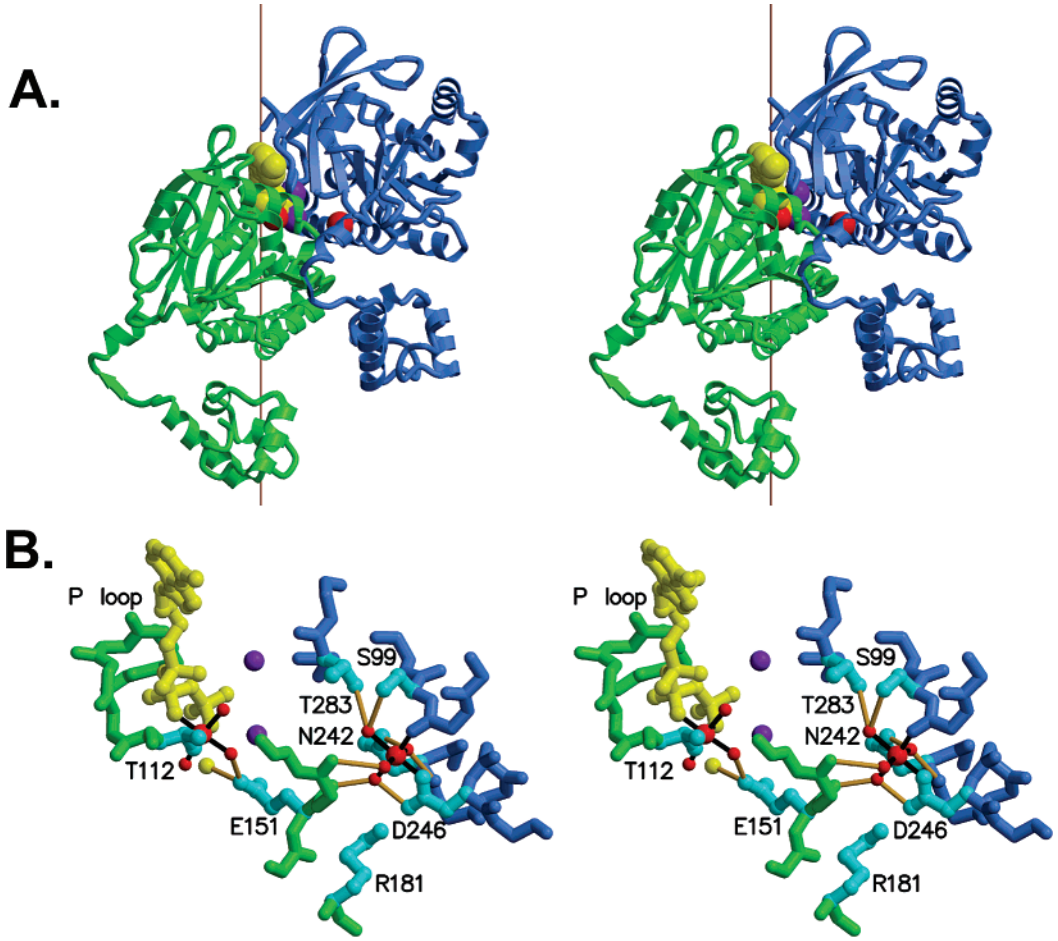

FIGURE 1: ATP and Mg^{2+} sites in stereo. One nonhydrolyzable ATP analogue AMP-PNP (yellow) and two Mg^{2+} (red spheres) have been located in the recently determined crystal structure of MvRadA (PDB code 2FPM). (A) Two neighboring MvRadA protomers are shown in green and blue, respectively. The filament axis is shown as a vertical line. Both Mg^{2+} ions are located at the subunit interface. Two K^+ ions (in purple) are located in the proximity of the γ-phosphate of the ATP analogue. (B) A magnified view showing the interactions with both Mg^{2+}. The viewing direction is identical to that of (A). Three water molecules liganding the AMP-PNP-bound Mg^{2+} as well as four water molecules liganding the secondary Mg^{2+} are shown in smaller red spheres. The putative hydrolyzing water is shown as a yellow sphere near the primary Mg^{2+} and the catalytic Glu-151. The coloring scheme for the main chain atoms is the same with that used in (A). Selected side chains are shown in cyan. The Mg^{2+}-liganding bonds are shown in black lines. Selected hydrogen bonds are shown in yellow lines. The secondary Mg^{2+} has a water ligand which interacts with the catalytic Glu-151. This figure was generated using Molscript (*37*) and Raster3D (*38*).

Mg^{2+} sites have been confirmed by anomalous scattering signals of a manganese-soaked crystal (*13*) and appear recurrent in other reported MvRadA structures in the ATPase-active conformation represented by the complex with the ATP analogue AMP-PNP and K^+ as well as in the ATPase-inactive conformation represented by the complex with ADP (*22*, *24*). The secondary Mg^{2+} is also buried at the subunit−subunit interface approximately 11 Å from the primary one. It is a formal possibility that the secondary divalent cation could affect the stability of active MvRadA filaments. Both cations exhibit typical octahedral coordination geometries (Figure 1B) as seen in many other protein structures containing Mg^{2+}. The secondary Mg^{2+} is coordinated by four water molecules (distances 2.0−2.2 Å), the main chain carbonyl of Gln-98 (2.0 Å), and the side chain carboxylate of Asp-246 (2.1 Å). Three of the four water ligands are also hydrogen-bonded with the polar side chains of Ser-99 (3.0 Å), Asn-242 (2.6 Å), and Asp-246 (2.6 Å), respectively (blue subunit, Figure 1B). The Ser-99 bridged water ligand also forms a weak hydrogen bond with the hydroxyl of Thr-283 (3.4 Å) in the ATPase-active conformation but does not in the ATPase-inactive conformation (4.4 Å apart; not shown). Across the subunit interface, the main chain carbonyl of the catalytic Glu-151 (green subunit, Figure 1B), which is equivalent to Glu-96 of EcRecA, also forms a hydrogen bond with the water ligand (2.6 Å) hydrogen-bonded with Asp-246. Nearby, the carbonyl of Gly-152 forms a weak hydrogen bond with the fourth water ligand (3.4 Å). The location of the secondary Mg^{2+} in the proximity of the catalytic Glu-151 implies a second formal possibility that the Mg^{2+} site could affect the ATPase activity of MvRadA by changing the conformation of Glu-151. Unlike the primary Mg^{2+} site which likely represents a P-loop-bound Mg-ATP^{2-} complex, the secondary Mg^{2+} does not appear to have any direct interaction with the ATP analogue. We reasoned that the secondary binding site would be sensitive to free Mg^{2+} rather than Mg-ATP^{2-} concentration. We therefore carried out strand exchange and ATPase assays in varied concentrations of Mg^{2+} to test these two possibilities. Our recent study (*23*) also suggests that Mg^{2+} could stimulate the strand exchange activity of MvRadA in the absence of K^+ or Ca^{2+} by possibly taking the role of either K^+ or Ca^{2+} in the promiscuous cation-binding pocket. However, in the presence of K^+, Mg^{2+} did not appear to compete for the

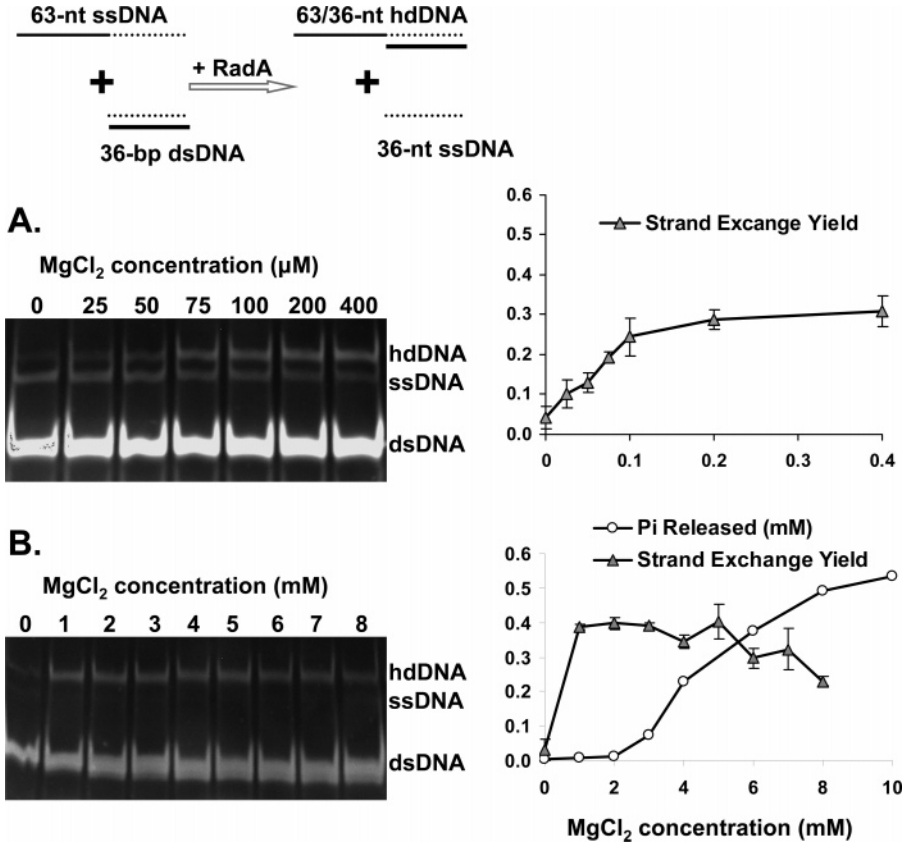

FIGURE 2: Mg^{2+}-dependent DNA strand exchange and ATP hydrolysis activities of MvRadA. The strand reaction scheme is shown in the top. The reaction solutions contained 5 mM ATP, 100 mM KCl, varied concentrations of $MgCl_2$, and 50 mM Hepes−Tris buffer at pH 7.4. The strand exchange reaction solutions also contained 21 μM wild-type MvRadA and 1 μM each of an ssDNA and a dsDNA substrate. Strand exchange activity was indicated by the formation of a slowest migrating heteroduplex DNA species (hdDNA). The acrylamide gels were stained by ethidium bromide, and its fluorescence signal was digitized for quantification. Yields and standard deviations derived from multiple strand exchange experiments are shown on the right. (A) Strand exchange reaction in the presence of low concentrations of $MgCl_2$. It appears that the strand exchange reaction requires the presence of ~50 μM Mg-ATP^{2-} for half-activation. (B) Strand exchange reaction in the presence of high concentrations of $MgCl_2$. The ATPase assays were performed in the same chemical solution but with 3 μM MvRadA and 0.5 μM poly$(dT)_{36}$. The concentration of released inorganic phosphate was measured after 30 min of reaction. The ATPase activity appears dormant until 3 mM or more $MgCl_2$ is present, while the strand exchange activity of wild-type MvRadA appears slightly decreased with increasing ATPase activity.

cation-binding pocket (see caveat below), therefore essentially enabling our interpretation of results based on a two-site model.

Strand Exchange Activity Is Sensitive to Mg-ATP^{2-} Concentration. The wild-type MvRadA has been observed to promote strand exchange between synthetic oligonucleotides in the presence of ATP or its hydrolysis-resistant analogues ATP-γ-S and AMP-PNP (*24*). In this assay, an MvRadA/ssDNA ratio of 1:3 was used, which follows the known stoichiometry for such recombinases. The acrylamide gel band corresponding to the heteroduplex product began to appear after 10 min, and its intensity reached a plateau after 30 min (time course data not shown). Therefore, a fixed reaction time of 30 min was chosen. We first verified the dependence of MvRadA on Mg-ATP^{2-} chelate as expected from the known cofactor requirement by RecA orthologues. A fixed overdose of ATP (5 mM) over $MgCl_2$ (0−0.4 mM) was used, such that the predominant majority of magnesium would exist as the Mg-ATP^{2-} complex (Figure 2A). The strand exchange yield gradually approached ~30% as total [$MgCl_2$], or [Mg-ATP^{2-}], increased to 0.4 mM. Expectedly, the apparent dissociation constant of MvRadA for Mg-ATP^{2-} was estimated to be 50 μM, a value in a similar range to those reported for known RecA orthologues.

Strand Exchange Activity Is Insensitive to Free Mg^{2+} Concentration. We further accessed the strand exchange activity of MvRadA in the presence of higher concentrations of $MgCl_2$ (1−8 mM) (Figure 2B). The yield stayed nearly constant around 35% with 1−5 mM $MgCl_2$ and slightly decreased with higher magnesium concentrations. In the presence of 8 mM $MgCl_2$, the yield decreased to ~20%. Since a constant ATP concentration of 5 mM was employed, the calculated free Mg^{2+} concentration varied by ~300-fold, ranging from 10 μM (corresponding to 1 mM total Mg^{2+}) to 3 mM (corresponding to 8 mM total Mg^{2+}). The activity change of less than 2-fold suggests that the strand exchange activity of MvRadA is insensitive to free Mg^{2+} concentration.

ATPase Activity Is Sensitive to Mg^{2+} Concentration. We also monitored the release of inorganic phosphate in 30 min as a crude measure of the rate of ATP hydrolysis (Figure 2B). An MvRadA/poly$(dT)_{36}$ (in nucleotides) ratio of 1:6 was used so as to achieve maximal stimulation of the ATPase activity of MvRadA. Little ATP was hydrolyzed in the presence of less than 2 mM $MgCl_2$. The extent of ATP hydrolysis sharply increased with 3 mM or more $MgCl_2$ and reached ~50% of the maximum when 4 mM $MgCl_2$ was present. It is worth noting that the ATPase activity of MvRadA is minimal in the absence of K^+. If Mg^{2+} could

compete with K^+ for the promiscuous cation-binding pocket, we would expect a sharp decrease in ATP hydrolysis. The results clearly showed a lack of such decrease, indicating that Mg^{2+} does not efficiently compete with K^+. It is not surprising that optimal strand exchange activities were observed under these low Mg^{2+} conditions (1−2 mM), since the Mg-ATP^{2-} complex is concentrated enough for saturating the ATPase site. As ATP is an Mg^{2+} chelator, the free Mg^{2+} concentration in the presence of 5 mM ATP must be significantly lower than the total concentration of $MgCl_2$. The lack of efficient ATP hydrolysis in 1−2 mM $MgCl_2$ is likely due to lower concentration of free Mg^{2+} rather than Mg-ATP^{2-} chelate. Using the MAXCHELATOR software (*25*), we tentatively assigned an apparent dissociation constant for the secondary Mg^{2+} as ∼0.2 mM, which corresponds to the free magnesium concentration in the presence of 4 mM $MgCl_2$ and 5 mM ATP. Since the secondary Mg^{2+}-binding site is close to the catalytic residue Glu-151, the dependence on the concentration of $MgCl_2$ implies that changes in the secondary site may propagate to the ATPase site.

Strand Exchange Activity Is Retained by the Asp-246 Mutant Proteins. Free magnesium ions appear to be needed for the activation of the ATPase activity of MvRadA but not for the activation of strand exchange activity. These results favor the possibility that the secondary Mg^{2+} serves as a switch for ATP hydrolysis while not significantly affecting filament stability. We further verified this assumption by mutating the Mg^{2+}-liganding Asp-246. An Asn as well as an Ala mutation was made. Lack of electron density in the secondary site of crystallized D246A protein suggests the loss of binding a second Mg^{2+} (Supporting Information). We presume the Asn mutant protein, though not successfully crystallized, would have similar properties due to the loss of the negatively charged carboxylate of residue 246. Compared with the wild-type protein, both mutant proteins exhibited higher yield (∼45%) in promoting DNA strand exchange (Figure 3A,B). It appears that the stability of the active recombinase assembly is not noticeably decreased by structural perturbation at the secondary Mg^{2+}-binding site. These results were similar to that of the wild-type protein in lower concentrations (1−2 mM) of $MgCl_2$. The crystal structures of MvRadA have provided a possible explanation to why stability is retained in the absence of the secondary Mg^{2+}. The Mg^{2+}-liganding Asp-246 also forms a hydrogen-bonded bridge with Arg-181 (Figure 1B), which is invariable in characterized RadA, Rad51, and DMC1 sequences. As such, the carboxylate of Asp-246 remains neutralized by Arg-181 even in the absence of magnesium, therefore avoiding a destabilizing scenario of burying this negatively charged group without neutralizing it.

ATPase Activity Is Markedly Reduced by Mutations at Mg^{2+}-Liganding Asp-246. Compared with the wild-type protein, the initial ATP turnover rates of the D246N and D246A proteins appeared noticeably reduced by ∼20-fold (Figure 3C). Their much-lowered ATPase activities are similar to that of the wild-type protein when little free Mg^{2+} is present. The possibility that binding the secondary Mg^{2+} is critical for ATPase activation is consistent with the location of this magnesium site near the catalytic residue Glu-151. The equivalent Glu-96 in EcRecA was first suggested as the general base to activate the nucleophile water (*26*). The

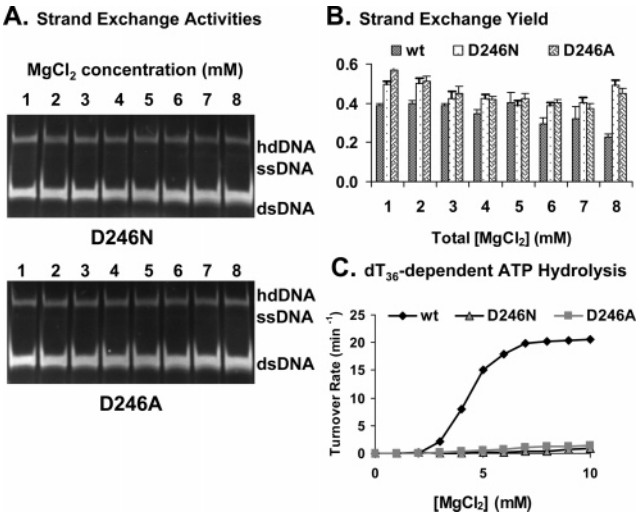

FIGURE 3: DNA strand exchange and ATP hydrolysis activities of mutant MvRadAs. (A) Strand exchange activity of the D246N and D246A mutant proteins in the presence of 5 mM ATP, 100 mM KCl, and 1−8 mM $MgCl_2$. (B) Quantified strand exchange yields of reactions in (A) and Figure 2. Standard deviations derived from multiple experiments are shown as error bars. (C) Turnover rates of ssDNA-dependent ATP hydrolysis in the presence of 5 mM ATP, 100 mM KCl, and 1−10 mM $MgCl_2$. Poly$(dT)_{36}$ was used as the ssDNA substrate. The D246N and D246A proteins are defective in ATP hydrolysis but proficient in strand exchange.

suggested role for this conserved Glu is consistent with the ATPase-active conformation of MvRadA (*22*), and the requirement for a precisely placed carboxylate general base was further supported by crystal structures of the E151D MvRadA protein and over 100-fold reduction in its ATPase activity (*19*). The observed hydrogen bond between the main chain carbonyl of Glu-151 and an Mg^{2+}-liganding water molecule (Figure 1B) may render the side chain of Glu-151 in a favorable state for catalyzing ATP hydrolysis. With the loss of this secondary Mg^{2+} ion, due to either an insufficient magnesium concentration or mutations at Asp-246, such a favorable state for catalysis likely becomes perturbed, therefore rendering the enzyme less effective. We could not rule out, however, the fact that the binding of a second Mg^{2+} at the subunit interface may speed up ADP/ATP exchange.

Promotion of Strand Exchange between Viron DNA. RecA orthologues are known to promote strand exchange between DNA substrates of several thousand nucleotides or base pairs in length. The much shorter (<100 nt/bp) synthetic DNA substrates may be of too little challenge to reveal filament destabilization. So as to rule out this possibility, we performed strand exchange assay using a circular single-stranded viron DNA (5386 nucleotides) and a linearized double-stranded viron DNA (5386 base pairs). The strand exchange reaction between the two homologous DNAs produced a nicked circular DNA species which migrated slower than the substrates (Figure 4). The low yield of less than 15% and poor reproducibility which led to 5−10% fluctuations prevented meaningful quantification. Nevertheless, the occurrence of a slower migrating product band on the agarose gels suggests that the wild-type and the Asp-246 mutant proteins are active in promoting extensive strand exchange. As observed in the exchange reaction between synthetic oligonucleotides, the strand exchange reaction between viron DNAs is not noticeably sensitive to free Mg^{2+} concentrations. Therefore, it is unlikely the secondary Mg^{2+},

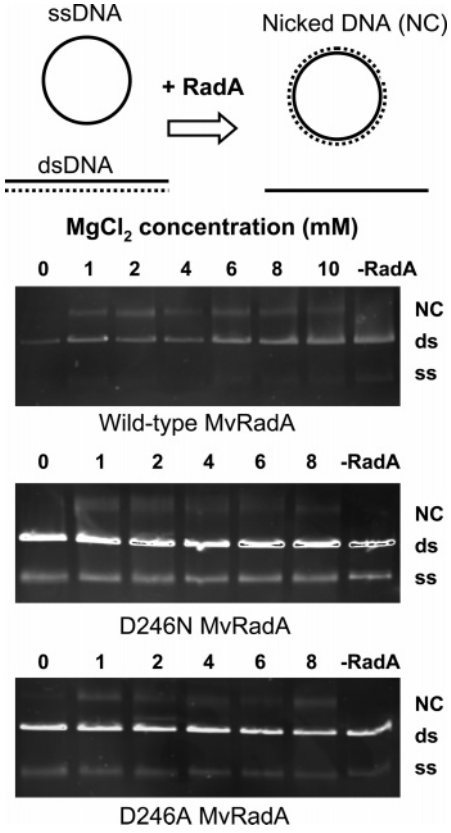

FIGURE 4: DNA strand exchange between virion DNAs. The strand reaction scheme is shown in the top. Strand exchange reactions were assayed in solutions containing 5 mM ATP, 100 mM KCl, specified concentrations of $MgCl_2$, 5 μM MvRadA, 1 μM *E. coli* SSB, 5 ng/μL circular ssDNA, and 10 ng/μL linear dsDNA. The product is the slowest migrating band of nicked circular DNA (NC) on the ethidium bromide-stained agarose gels. The wild-type MvRadA and the D246N and D246A mutant proteins are similarly active in promoting extensive strand exchange.

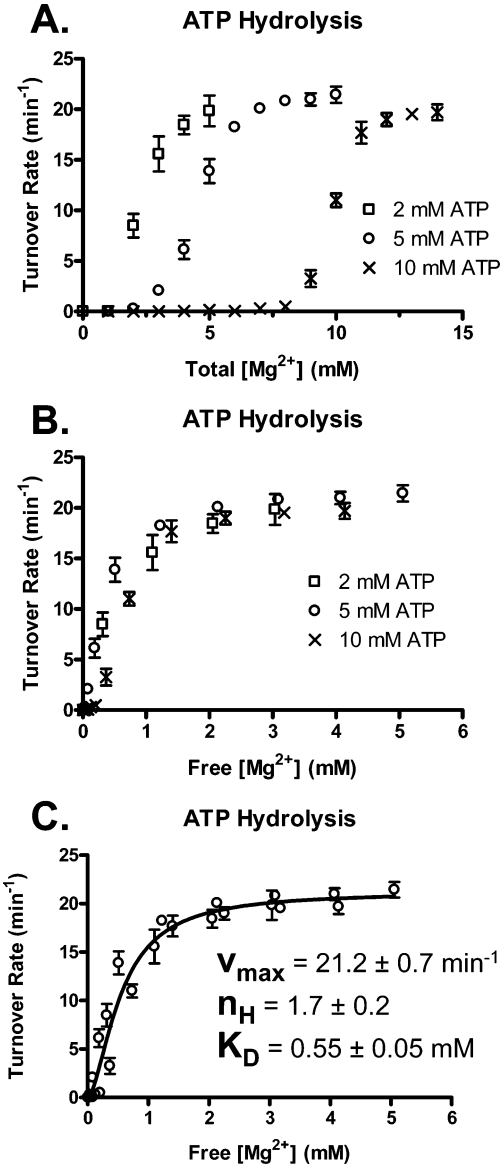

FIGURE 5: Kinetic parameters of ATP hydrolysis. The turnover rates of the ATP hydrolysis reaction were derived by monitoring the initial time course of phosphate release (within the first 15 min). The standard errors (shown as vertical bars) were derived from three repeated experiments. The reaction solutions contained 100 mM KCl, varied concentrations of $MgCl_2$, three specified concentrations of ATP, 3 μM wild-type MvRadA, and 0.5 μM poly(dT)$_{36}$. (A) Turnover rates versus total Mg^{2+} concentrations. The rate drastically increases as the $MgCl_2$ concentration surpasses the ATP concentration. (B) Turnover rates versus free Mg^{2+} concentrations. The trends with three ATP concentrations appear correlated. (C) Kinetic parameters of the reaction derived by nonlinear fitting using the Prism software (GraphPad).

despite being located at the subunit interface, would significantly affect the formation and stability of the strand exchange-active nucleoprotein filaments.

Kinetic Parameters of ATP Hydrolysis Catalyzed by MvRadA. Only the ATPase activity of MvRadA appears to be sensitive to the concentration of free Mg^{2+}. We further verified this conclusion by using three different ATP concentrations (2, 5, 10 mM). As expected, the turnover rate sharply increased when total $MgCl_2$ concentrations approached the concentration of the Mg^{2+}-chelating ATP (Figure 5A). Using the MAXCHELATOR software to estimate free Mg^{2+} concentrations, the trends of turnover rates in three different concentrations of ATP against the concentration of free Mg^{2+} but not total Mg^{2+} appeared to be correlated (Figure 5A,B). To derive kinetic parameters of the ATP hydrolysis reaction, we further employed nonlinear curve fitting with the Prism software (GraphPad) using all measured rates against calculated concentrations of free Mg^{2+} (Figure 5C). The maximum turnover rate was estimated to be 21.2 $\pm$ 0.7 min^{-1}, and the dissociation constant for the secondary Mg^{2+} was estimated to be 0.55 $\pm$ 0.05 mM. The Hill coefficient was estimated to be 1.7 $\pm$ 0.2, indicating a low level of cooperativity similar to other characterized Rad51/RadA homologues (*27*, *28*). Changes in the secondary Mg^{2+} site in the D246A structure does not appear to cause gross changes in the neighboring subunit, therefore providing an explanation to the lack of apparent cooperativity. Strikingly unlike EcRecA, Rad51/DMC1/RadA proteins lack a high level of cooperativity on the binding of Mg-ATP^{2-}. Though no structural evidence has been gained on an MvRadA filament with mixed ATP and ADP occupancy, existing structures of MvRadA indicate that ATP-bound and ADP-bound filaments are strikingly similar in helical parameters (*24*). It is possible MvRadA filaments could tolerate the binding of ATP and ADP in neighboring ATPase centers, rendering such filaments noncooperative.

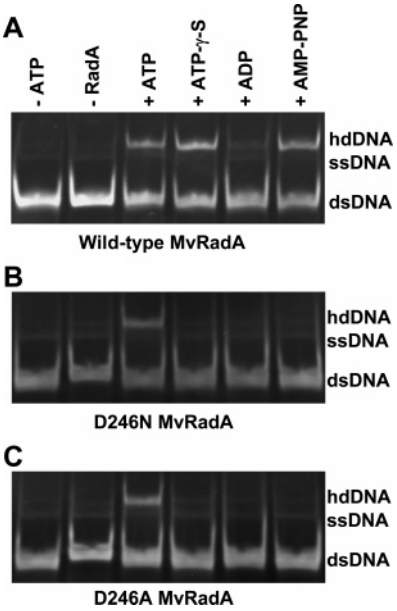

FIGURE 6: Selectivity on nucleotide substrates. The strand exchange reaction scheme as well as protein and DNA concentrations is identical to that in Figure 2. The reaction solution contained 10 mM $MgCl_2$, 100 mM KCl, and 5 mM specified nucleotide. The wild-type protein is active in the presence of ATP, ATP-γ-S, and AMP-PNP (A). The D246N (B) and the D246A (C) mutant proteins are active only in the presence of ATP.

Selectivity on Nucleotide Substrates. The recent study by Fishel and co-workers on human Rad51 has demonstrated that magnesium affects ATP/ADP selection (*16*). In other words, change in the ATPase center is induced by magnesium. The MvRadA orthologue's ATPase activity appears to be affected by binding of a secondary Mg^{2+} not directly associated with the ATP substrate. We further probed nucleotide substrate selectivity of the MvRadA-promoted strand exchange reaction between homologous oligonucleotides. The wild-type MvRadA exhibited comparable strand exchange activity in the presence of ATP as well as analogous AMP-PNP and ATP-γ-S (Figure 6A). In contrast, the strand exchange activity of the two mutant proteins with a site-directed mutation at the secondary Mg^{2+}-liganding Asp-246 exhibited marked preference for ATP over the two nonhydrolyzable ATP analogues (Figure 6B,C). These results again suggest that changes in the secondary Mg^{2+}-binding site propagate to the ATPase center to enable distinguishing between ATP and its analogues. Recently reported structures of MvRadA in the presence of AMP-PNP and an activating dose of K^+ or Ca^{2+} have revealed an active conformation in which the DNA-interacting L2 region is largely ordered. On the other hand, MvRadA structures in the presence of ADP or in the presence of AMP-PNP but lacking an activating cation have recurrently revealed an inactive conformation with a largely disordered L2 region. Since the D246A protein cannot utilize AMP-PNP as a cofactor to promote strand exchange, it is not surprising, after all, that the crystal structure of this mutant protein in complex of AMP-PNP and K^+ was observed in the inactive form (Supporting Information).

DISCUSSION

The archaeal RadA protein from *M. voltae* is a bona fide RecA orthologue that promotes extensive strand exchange between homologous DNAs. As expected from an ATPase with a P-loop that binds Mg-ATP^{2-} chelate, the activation of this recombinase requires the presence of both Mg^{2+} and ATP. Despite the intersubunit location of the secondary Mg^{2+}, the strand exchange activity of MvRadA does not appear to be sensitive to free Mg^{2+} concentration. This implies that binding a secondary Mg^{2+} would not significantly affect the assembly of active recombinase−DNA filaments. On the other hand, the ATPase activity of MvRadA appears to be sensitive to free Mg^{2+} concentration. Besides, the preference for nucleotide cofactors appears to be altered by site-directed mutagenesis at the Mg^{2+}-liganding Asp-246. The ATPase observations along with the location of the secondary Mg^{2+} in the proximity of the catalytic Glu-151 collectively suggest that the secondary Mg^{2+}-binding site serves as an allosteric switch for ATP hydrolysis. The marine habitat of *M. voltae* has a relatively high Mg^{2+} concentration around 50 mM. A study shows that marine bacteria enrich magnesium by 10−20-fold (*29*). Adding the fact that CorA magnesium intake systems are ubiquitous in archaea (*30*), it seems likely that this marine organism maintains an adequately high intracellular Mg^{2+} concentration to activate the ATPase activity of MvRadA. Though unlikely to be conserved in the intensively studied EcRecA due to large differences in amino acid sequence, a similar divalent cation-binding site may exist in some closely related eukaryal orthologues. Human and yeast Rad51s do have a conserved Asp residue at their respective equivalent positions of residue 246 of MvRadA. Interestingly, the activity of human is sensitive of Mg^{2+} concentration (*15*) which has been further addressed to Mg^{2+}-affected selection of ATP over ADP at the ATPase center (*16*). Unlike human Rad51, the strand exchange activity of MvRadA is insensitive to Mg^{2+} concentration. Nonetheless, mutations at Asp-246 of the archaeal orthologue exhibit altered preference for nucleotide cofactors, further indicating allosteric communication between the secondary Mg^{2+} site and the ATPase center.

An active recombinase−DNA filament is in a strand exchange-competent state which harbors an extended and underwound form of DNA as compared with B-DNA (*31*). The active filament dissembles by its intrinsic ATPase activity unless ATP hydrolysis is blocked or ATP is replenished by ADP/ATP exchange. The severe toxicity by a E96D mutation in EcRecA appears to suggest that ATPase activity appears to be functionally important in releasing DNA. Human Rad51 and other eukaryote orthologues appear to be inefficient in hydrolyzing ATP. Unlike the E96D mutant of EcRecA, such inefficiency by eukaryote recombinases does not cause cytotoxicity. For human Rad51, its inefficiency in ATP hydrolysis is partly due to slow ADP/ATP exchange and can be accelerated by hXRCC2 (*32*). It is worth noting that a high concentration of Mg^{2+} further deactivates human Rad51 by blocking ADP/ATP exchange (*16*). Another divalent cation, Ca^{2+}, has recently been demonstrated to inhibit ATP hydrolysis and elevate strand exchange activity of human Rad51 (*33*). Similar stimulatory effects by Ca^{2+} have also been reported for human DMC1, yeast Rad51, and archaeal RadA (*23*, *34*, *35*). Recently, the stimulatory roles by monovalent cations such as K^+ and larger M^+ on human Rad51 have been systematically studied (*36*), and similar stimulation by K^+ on MvRadA has been

structurally rationalized (*19*, *22*). Such divalent and monovalent stimulants exert their stabilization on an active conformation by filling a promiscuous cation-binding pocket near the γ-phosphate of ATP. In this study, we further studied the secondary Mg^{2+}-binding site of MvRadA, which is located between subunits and in the proximity of the catalytic glutamate (Glu-151). Such a location is ideal for exerting allosteric effects on filament assembly and/or ATP hydrolysis. Our results suggest it is the latter of MvRadA that is affected by Mg^{2+} binding. On the basis of the observed over 100-fold reduction in ATPase rate by substituting Glu-151 for an Asp (*19*), the precise positioning of the catalytic carboxylate appears to be required for efficient ATP hydrolysis. The secondary Mg^{2+} could stabilize such positioning of the carboxylate by water-bridged interactions with Glu-151 as seen in MvRadA structures. Interestingly, this site has also been found to bind Ca^{2+} (*23*). We argue that the structural element for binding free Mg^{2+} or even Ca^{2+} may be shared by some members of this group of archaeal and eukaryal recombinases due to the conservation of Asp-246. Unlike bacteria and archaea, in which RecA and RadA proteins are likely concurrently active in ATP hydrolysis and DNA strand exchange, eukaryal orthologues appear at least an order of magnitude slower in hydrolyzing ATP, a step required for releasing DNA after strand exchange. In theory, signaling and protein−protein interactions such as the stimulating interactions by human XRCC2 on Rad51 (*32*) could offer a way of regulated ATP hydrolysis and subsequent DNA release in multicellular organisms. Though a possible signaling role played by divalent cations has never been established by in vivo experiments, the physiological relevance of M^{2+}-binding sites in eukaryal recombinases warrants further study so as to arrive at a comprehensive understanding of the assembly and life span of active recombinase−DNA filaments.

ACKNOWLEDGMENT

We thank Drs. Gabriele Schatte and Wilson Quail at the Saskatchewan Structural Sciences Centre for assistance to the Proteum-R X-ray facility.

SUPPORTING INFORMATION AVAILABLE

Crystal structure determination of D246A MvRadA and one figure showing lack of electron density for a second Mg^{2+}. This material is available free of charge via the Internet at http://pubs.acs.org.

REFERENCES

1. Cox, M. M. (1998) A broadening view of recombinational DNA repair in bacteria, *Genes Cells 3*, 65−78.
2. Cox, M. M., Goodman, M. F., Kreuzer, K. N., Sherratt, D. J., Sandler, S. J., and Marians, K. J. (2000) The importance of repairing stalled replication forks, *Nature 404*, 37−41.
3. Courcelle, J., Ganesan, A. K., and Hanawalt, P. C. (2001) Therefore, what are recombination proteins there for?, *BioEssays 23*, 463−470.
4. Lusetti, S. L., and Cox, M. M. (2002) The bacterial RecA protein and the recombinational DNA repair of stalled replication forks, *Annu. Rev. Biochem. 71*, 71−100.
5. Kowalczykowski, S. C. (2000) Initiation of genetic recombination and recombination-dependent replication, *Trends Biochem. Sci. 25*, 156−165.
6. Seitz, E. M., and Kowalczykowski, S. C. (2000) The DNA binding and pairing preferences of the archaeal RadA protein demonstrate a universal characteristic of DNA strand exchange proteins, *Mol. Microbiol. 37*, 555−560.
7. Clark, A. J., and Margulies, A. D. (1965) Isolation and characterization of recombination-deficient mutants of *Escherichia coli* K12, *Proc. Natl. Acad. Sci. U.S.A. 53*, 451−459.
8. Sandler, S. J., Satin, L. H., Samra, H. S., and Clark, A. J. (1996) recA-like genes from three archaean species with putative protein products similar to Rad51 and Dmc1 proteins of the yeast *Saccharomyces cerevisiae*, *Nucleic Acids Res. 24*, 2125−2132.
9. Shinohara, A., Ogawa, H., and Ogawa, T. (1992) Rad51 protein involved in repair and recombination in *S. cerevisiae* is a RecA-like protein, *Cell 69*, 457−470.
10. Bishop, D. K., Park, D., Xu, L., and Kleckner, N. (1992) DMC1: a meiosis-specific yeast homolog of *E. coli* recA required for recombination, synaptonemal complex formation, and cell cycle progression, *Cell 69*, 439−456.
11. VanLoock, M. S., Yu, X., Yang, S., Lai, A. L., Low, C., Campbell, M. J., and Egelman, E. H. (2003) ATP-mediated conformational changes in the RecA filament, *Structure (Cambridge) 11*, 187−196.
12. Conway, A. B., Lynch, T. W., Zhang, Y., Fortin, G. S., Fung, C. W., Symington, L. S., and Rice, P. A. (2004) Crystal structure of a Rad51 filament, *Nat. Struct. Mol. Biol. 11*, 791−796.
13. Wu, Y., He, Y., Moya, I. A., Qian, X., and Luo, Y. (2004) Crystal structure of archaeal recombinase RadA, a snapshot of its extended conformation, *Mol. Cell 15*, 423−435.
14. Lusetti, S. L., Shaw, J. J., and Cox, M. M. (2003) Magnesium ion-dependent activation of the RecA protein involves the C terminus, *J. Biol. Chem. 278*, 16381−16388.
15. Baumann, P., and West, S. C. (1997) The human Rad51 protein: polarity of strand transfer and stimulation by hRP-A, *EMBO J. 16*, 5198−5206.
16. Shim, K. S., Tombline, G., Heinen, C. D., Charbonneau, N., Schmutte, C., and Fishel, R. (2006) Magnesium influences the discrimination and release of ADP by human RAD51, *DNA Repair (Amsterdam) 5*, 704−717.
17. Higuchi, R., Krummel, B., and Saiki, R. K. (1988) A general method of in vitro preparation and specific mutagenesis of DNA fragments: study of protein and DNA interactions, *Nucleic Acids Res. 16*, 7351−7367.
18. Ho, S. N., Hunt, H. D., Horton, R. M., Pullen, J. K., and Pease, L. R. (1989) Site-directed mutagenesis by overlap extension using the polymerase chain reaction, *Gene 77*, 51−59.
19. Qian, X., He, Y., Wu, Y., and Luo, Y. (2006) Asp302 determines potassium dependence of a RadA recombinase from *Methanococcus voltae*, *J. Mol. Biol. 360*, 537−547.
20. Itaya, K., and Ui, M. (1966) A new micromethod for the colorimetric determination of inorganic phosphate, *Clin. Chim. Acta 14*, 361−366.
21. Mazin, A. V., Zaitseva, E., Sung, P., and Kowalczykowski, S. C. (2000) Tailed duplex DNA is the preferred substrate for Rad51 protein-mediated homologous pairing, *EMBO J. 19*, 1148−1156.
22. Wu, Y., Qian, X., He, Y., Moya, I. A., and Luo, Y. (2005) Crystal structure of an ATPase-active form of Rad51 homolog from *Methanococcus voltae*. Insights into potassium dependence, *J. Biol. Chem. 280*, 722−728.
23. Qian, X., He, Y., Ma, X., Fodje, M. N., Grochulski, P., and Luo, Y. (2006) Calcium stiffens archaeal Rad51 recombinase from *Methanococcus voltae* for homologous recombination, *J. Biol. Chem. 281*, 39380−39387.
24. Qian, X., Wu, Y., He, Y., and Luo, Y. (2005) Crystal structure of *Methanococcus voltae* RadA in complex with ADP: hydrolysis-induced conformational change, *Biochemistry 44*, 13753−13761.
25. Patton, C., Thompson, S., and Epel, D. (2004) Some precautions in using chelators to buffer metals in biological solutions, *Cell Calcium 35*, 427−431.
26. Story, R. M., Weber, I. T., and Steitz, T. A. (1992) The structure of the *E. coli* recA protein monomer and polymer, *Nature 355*, 318−325.
27. Tombline, G., and Fishel, R. (2002) Biochemical characterization of the human RAD51 protein. I. ATP hydrolysis, *J. Biol. Chem. 277*, 14417−14425.
28. Kil, Y. V., Glazunov, E. A., and Lanzov, V. A. (2005) Characteristic thermodependence of the RadA recombinase from the hyperthermophilic archaeon *Desulfurococcus amylolyticus*, *J. Bacteriol. 187*, 2555−2557.

29. Fagerbakke, K. M., Norland, S., and Heldal, M. (1999) The inorganic ion content of native aquatic bacteria, *Can. J. Microbiol. 45*, 304−311.
30. Kehres, D. G., Lawyer, C. H., and Maguire, M. E. (1998) The CorA magnesium transporter gene family, *Microb. Comp. Genomics 3*, 151−169.
31. Egelman, E. H. (2001) Does a stretched DNA structure dictate the helical geometry of RecA-like filaments?, *J. Mol. Biol. 309*, 539−542.
32. Shim, K. S., Schmutte, C., Tombline, G., Heinen, C. D., and Fishel, R. (2004) hXRCC2 enhances ADP/ATP processing and strand exchange by hRAD51, *J. Biol. Chem. 279*, 30385−30394.
33. Bugreev, D. V., and Mazin, A. V. (2004) Ca^{2+} activates human homologous recombination protein Rad51 by modulating its ATPase activity, *Proc. Natl. Acad. Sci. U.S.A. 101*, 9988−9993.
34. Bugreev, D. V., Golub, E. I., Stasiak, A. Z., Stasiak, A., and Mazin, A. V. (2005) Activation of human meiosis-specific recombinase Dmc1 by Ca^{2+}, *J. Biol. Chem. 280*, 26886−26895.
35. Lee, M. H., Chang, Y. C., Hong, E. L., Grubb, J., Chang, C. S., Bishop, D. K., and Wang, T. F. (2005) Calcium ion promotes yeast Dmc1 activity via formation of long and fine helical filaments with single-stranded DNA, *J. Biol. Chem.*
36. Shim, K. S., Schmutte, C., Yoder, K., and Fishel, R. (2006) Defining the salt effect on human RAD51 activities, *DNA Repair (Amsterdam) 5*, 718−730.
37. Kraulis, P. (1991) MOLSCRIPT: a program to produce both detailed and schematic plots of protein structures, *J. Appl. Crystallogr. 24*, 946−950.
38. Bacon, D. J., and Anderson, W. F. (1988) A fast algorithm for rendering space-filling molecule pictures, *J. Mol. Graphics 6*, 219−220.

BI6024098